MWR-824 (DJ) Schultz revision 9/5/03

Snowbands during the Cold-Air Outbreak of 23 January 2003

DAVID M. SCHULTZ

Cooperative Institute for Mesoscale Meteorological Studies, The University of Oklahoma and NOAA/National Severe Storms Laboratory, Norman, Oklahoma

DEREK S. ARNDT

Oklahoma Climatological Survey, The University of Oklahoma, Norman, Oklahoma

DAVID J. STENSRUD

NOAA/National Severe Storms Laboratory, Norman, Oklahoma

JAY W. HANNA

NOAA/NESDIS Satellite Services Division, Camp Springs, Maryland

Monthly Weather Review
PICTURE OF THE MONTH

Submitted: 12 May 2003
Revised: 5 September 2003

Corresponding author address: Dr. David M. Schultz, NOAA/NSSL, 1313 Halley Circle, Norman, OK 73069. Email: david.schultz@ noaa.gov

ABSTRACT

A cold-air outbreak east of the Rocky Mountains on 23 January 2003 produced banded clouds and snow across the central and southeastern United States. The bands occurred through two processes: 1) thermal instability in the planetary boundary layer produced horizontal convective rolls (HCRs) over widespread areas and, 2) lake-effect processes downstream of small lakes (fetch<100 km) produced localized bands. Characteristics of the observed bands associated with the HCRs, such as horizontal scale, depth of circulation, orientation, duration, and dynamics, are explored through observations, previous literature, and theoretical models. Snow from clouds produced by HCRs over land during the cold season has not been extensively studied previously. In this event, cold-air advection over the warm ground led to an upward sensible heat flux, promoting the occurrence of the HCR circulations. As the surface temperature decreased, the height of the lifting condensation level decreased, eventually forming cloud bands within the ascending portion of the HCR circulations. Ice crystals are inferred to have fallen from a large-scale precipitation system aloft into the cloud bands in the planetary boundary layer, which was within the favored temperature regime for dendritic growth of ice crystals. The ice crystals grew and reached the surface as light snow. This seeder–feeder process suggests one way to anticipate development of such snowbands in the future, as demonstrated by other similar events on other days in Oklahoma and Illinois. As the cloud bands were advected equatorward, they ingested drier air and dissipated. Among the several lake-effect bands observed on 23 January 2003, one notable band occurred downwind of Lake Kentucky. Midlake convergence of the land breeze may have initially produced a narrow cloud band, which broadened as the land breeze ended. That the snowbands due to the HCRs and lake effect were both associated with heat and/or

moisture fluxes from the Earth's surface highlights the potential importance of ground- and water-surface temperature measurements for accurate numerical weather prediction.

1. Introduction

On the morning of 23 January 2003, an anticyclone with a central pressure of 1048 hPa moved equatorward east of the Rocky Mountains (Fig. 1), bringing the coldest air of the winter south and east. Several stations set record cold low temperatures for the day (–31.1°C/–24°F at Huron, SD, and –22.8°C /–9°F at Kansas City, MO); others set record cold high temperatures for the day (–11.1°C/12°F at Paducah, KY, and –6.1°C/21°F at Huntsville, AL). Although a coastal low was dumping up to a foot (30 cm) of snow in North Carolina (Fig. 1), skies were generally clear farther west, except for a few light snow flurries. Despite accumulations from these snow flurries ranging from a dusting to less than an inch (2.5 cm), at least three National Weather Service (NWS) forecast offices (Springfield, MO; Norman, OK; and Huntsville, AL) mentioned the snow in their Area Forecast Discussion products after it had already begun falling. Specifically, two of these offices attributed them to lake-effect processes, such as those that occur with the Great Lakes (e.g., Niziol 1987; Niziol et al. 1995). The operational Eta model initialized at 0000 UTC 23 January did not generate this snow (not shown).

As we discussed this event during the daily afternoon Storm Prediction Center–National Severe Storms Laboratory weather discussion (Kain et al. 2003), we recognized that, although some snows were found locally downstream of lakes, most of the snow showers were organized over a much larger area. The widespread existence of these snow showers can be seen from the bands in the unfiltered, 0.5° elevation angle, WSR-88D radar reflectivity factor (Fig. 2) and *GOES-8* longwave-infrared (channel 4) satellite imagery (Fig. 3). For example, at their most widespread around 1000 UTC, the bands covered an area at least 600 km x 500 km. [For an animation of these and other graphics in this paper, see http://www.cimms.ou.edu/~schultz/hcr/.] Over time, the location of the region encompassing the bands moved south and east from Kansas and Missouri at 2346 UTC 22 January (Fig. 2a); Oklahoma, Arkansas, Kentucky, Illinois, and Tennessee at 0604 UTC 23 January (Fig. 2b); Mississippi, Alabama, Georgia, and Tennessee at 1152 UTC 23 January (Fig. 2c); to Tennessee and North Carolina at 1515 UTC 23 January (Fig. 2d). The regular spacing of the bands over such a widespread area clearly indicates that they were not a local phenomenon like lake effect. In addition, the bands in Fig. 2 were only detected close to the radar, indicating that they were relatively shallow boundary-layer features.

Several mechanisms for these bands are possible. Gravity waves above convectively active boundary layers have been observed by Kuettner et al. (1987) and modeled by Clark et al. (1986). The long-lived north–south-oriented bands in this case could not have been gravity waves because they remained nearly stationary with the wind blowing parallel to the long axis of the majority of the bands, not across the bands as would have been expected for gravity waves. These bands could not have been due to conditional symmetric instability (e.g., Schultz and Schumacher 1999), since they were not aligned nearly perpendicular to the thermal wind. A boundary-layer circulation called horizontal convective rolls, however, is a strong possibility since the bands were associated with a strong cold-air outbreak, were regularly spaced over a large area, and occurred within the planetary boundary layer. Thus, a working hypothesis is that horizontal convective rolls (HCRs) may be associated with band formation in this case. In the rest of this section, we provide some background information on HCRs.

If sufficiently deep and moist, the updrafts associated with HCRs in the planetary boundary layer can saturate and produce parallel cloud bands (or cloud streets), which can be a common occurrence in the atmosphere (e.g., Kuettner 1959, 1971; Atkinson and Zhang 1996; Weckwerth et al. 1997; Young et al. 2003). The mechanisms that lead to HCR development can be grouped into either thermal or dynamic instabilities. Because the event on 23 January 2003 was associated with cold continental air flowing over a relatively warm land surface, the thermal-instability mechanism is a likely candidate. For such a mechanism, buoyancy provides the energy for the circulations, and the vertical wind shear organizes the circulations into bands such that the shear is minimized in the cross-band direction (e.g., Kuo 1963; Asai 1970; Shirer 1986). Consequently, HCRs due to the thermal-instability mechanism often are observed in slightly unstable environments with some sensible heat flux from the surface (e.g., Table 1 in Atkinson and Zhang 1996; Weckworth et al. 1997). As environmental instability increases, however, the likelihood of such two-dimensional rolls being the dominant form of convective organization decreases for a given wind shear (Krishnamurti 1975; Grossman 1982).

HCRs are relatively common over land during the warm season [see Atkinson and Zhang (1996), Weckwerth et al. (1997), and Young et al. (2002) for reviews] and over water during the cold season (e.g., Kuettner 1959, 1971; Holroyd 1971; Brown 1980; Walter 1980; Kelly 1982,1984; Miura 1986; Shirer and Brümmer 1986; Kristovich 1993). In contrast, relatively little has been written about HCRs that begin and end over land during the cold season. For example, Kuettner (1937) described cloud bands that formed when arctic air moved over northern Scandinavia after the land was heated during the long summer days, and Maletzke (1953) noted the frequent occurrence of bands over the central United States in outbreaks of polar continental air. Ligda and Bigler (1958) observed bands in radar imagery behind two cold fronts over southern Texas. Snow from HCRs over land is even rarer, as documented precipitating cold-season HCRs are generally lake-effect snowbands that occur over and downstream of lakes (Holroyd 1971; Kelly 1982; Kristovich 1993). Thus, the 23 January 2003 event warrants further examination due to its novelty as a possible snow-producing HCR event over land. The purpose of this paper is to explore in more detail the characteristics, nature, and occurrence of these circulations and their associated snowbands.

2. Snowbands likely associated with horizontal convective rolls

In this section, we explore the dimensions, orientations, duration, dynamics of the bands, as well as the processes that produce snow within them. Finally, we briefly mention other recent cold-season snowband events similar to the 23 January 2003 event.

a. Dimensions and orientations of the rolls

Radar and satellite imagery indicate the bands were 50–350 km long by about 10 km wide and spaced about 10–30 km apart (Figs. 2 and 3). Most of the bands were nearly linear with a roughly constant length and width, although some bands were less so (i.e., over Oklahoma in Figs. 2b and 3b). Others with smaller wavelengths formed over the crest of the Appalachian Mountains (e.g., Fig. 3d). It is possible that the topography, either directly (e.g., gravity waves) or indirectly (e.g., modification of the planetary boundary layer), played a role in those particular bands, but that is not investigated here. The rest of the paper deals with the large areas of bands over the central and southeastern United States (Figs. 2 and 3).

Because the bands were detected only within about 100 km from the radar (Fig. 2), the 0.5°-elevation-angle radar beam likely overshot the band beyond that distance. The online WSR-88D beam-characteristics calculator (http://www.wdtb.noaa.gov/resources/misc/beamwidth/index.htm) indicates that the bottom of the 0.5°-elevation-angle radar beam at a range of 100 km would be 660 m above radar level. Soundings from sites within the regions of active bands show that the top of the shallow surface mixed layer was typically 450–1000 m above the ground and capped by a strong frontal inversion (e.g., Fig. 4). These results affirm that the bands occurred within or near the top of the planetary boundary layer.

HCRs in the planetary boundary layer form when the environmental lapse rate is near neutral or slightly unstable, the mean wind speed in the roll layer exceeds some relatively small value (2–5 m s^{-1}), the vertical wind shear is nonzero, and a modest value of surface sensible heat flux exists (e.g., Atkinson and Zhang 1996; Weckwerth et al. 1997, and references therein). Soundings taken at locations where the snowbands were observed indicate that the environmental lapse rates within the boundary layer were neutral or slightly unstable, the mean wind speed in the boundary layer was above 5 m s^{-1}, and the vertical wind shear was nonzero (Fig. 4). Thus, the basic characteristics of the observed soundings were at least supportive of the notion that these bands may have been associated with HCRs.

Another parameter to characterize the bands is the aspect ratio $A=L/h$, where L is the spacing between the cloud bands (wavelength) and h is the depth of the circulation, often taken to be the depth of the planetary boundary layer. Previously published values of A for HCRs are generally 1–10 (e.g., Kelly 1984; Miura 1986; Atkinson and Zhang 1996; Young et al. 2003), with values occasionally as high as 30–40 (e.g., Holroyd 1971; LeMone and Meitín 1984). Unfortunately, high-temporal resolution soundings were not available during the 23 January snowbands, so the temporal variations of h (and hence, A) were unable to be determined. Where the depth of the planetary boundary layer, h, could be determined from soundings coincident with the presence of bands, A ranged between 15 and 40, values that are on the high end of those in previous studies. If the bands on 23 January 2003 were due to HCRs, one possible reason for these large aspect ratios was cell broadening.

Cell broadening may be due to a number of processes: the interactions between HCRs and gravity waves in the free atmosphere (Clark et al. 1986), the influence of poorly conducting boundaries (Sasaki 1970), the anisotropy of eddy diffusion (Agee 1976), latent heat release (Helfand and Kalnay 1983), and the more efficient vertical transport of heat (Atlas et al. 1983; Chang and Shirer 1984). The initial HCR circulations on 23 January 2003 likely occurred in clear air as the colder air first reached the region of warm land surface temperatures. Consequently, the wavelength, and hence aspect ratio, when the circulations first formed were unfortunately unknown. Once the circulations appeared on radar, their wavelength increased over time. The snowband spacing over south-central Kansas increased from 17 km at 2258 UTC 22 January to 24 km at 0113 UTC 23 January (not shown). Similarly, the snowband spacing over north-central Tennessee increased from 21 km at 0956 UTC 23 January to 37 km at 1054

UTC 23 January (not shown). The latter example suggests that the boundary layer would have had to deepen by 76% in about an hour in order for the aspect ratio not to have increased, a change that was not supported at other sounding locations (e.g., Fig. 4c) and was unlikely with the strong stability of the inversion at the top of the boundary layer. Thus, the large aspect ratios and the observed cell broadening in the present case were consistent with the typical evolution of HCRs in which the aspect ratio of the rolls increased both as the depth of the boundary layer and wavelength increased (Atlas et al. 1983; Muira 1986).

To investigate the variations in the orientation of the bands, locations where bands occurred that had simultaneous radiosonde soundings were investigated. There were four stations satisfying these criteria (Table 1). The orientation of the bands varied from nearly east–west at Dodge City, Kansas (DDC) to northeast–southwest at Wichita, Kansas (KICT) to nearly north–south in Alabama and Mississippi (Fig. 2). If thermal instability was the dominant mechanism for HCR development, the band orientation angle could be predicted based upon minimizing the wind shear perpendicular to the roll circulation (e.g., Kuo 1963; Asai 1970), as shown in the low-order spectral model of Shirer (1986). Using Shirer's (1986, his equation 3.13) analytic expression for roll orientation, good agreement is found between the predicted and observed roll orientations, with errors of only 8–19° (Table 1). The orientation of bands over Dodge City was particularly noteworthy---the winds were generally northerly, except for a slight cyclonic turning of the winds with height within the planetary boundary layer (Fig. 4b), producing a roughly east–west-oriented vertical wind shear. Thus, the cloud bands on 23 January 2003 were oriented to minimize the wind shear in the cross-roll direction, as expected from HCR theory. Significantly, this shear produced east–west band orientations, which were dramatically different from the northerly mean wind in the planetary boundary layer (Fig. 4b). Some studies advocate that HCRs should lie within 20° of the mean wind direction [discussed on p. ES62 in Young et al. (2003)]. In such cases, the wind is typically unidirectional with height such that the wind shear is in the same direction as the mean wind. The bands in the vicinity of Dodge City demonstrate that the band orientation does not necessarily have to be in the same direction as the mean wind.

It is also possible that the bands in the vicinity of Dodge City may have been due to gravity waves (e.g., Clark et al. 1986; Kuettner et al. 1987) since their orientation was perpendicular to the mean wind. In addition, the stable layer between 850 and 700 hPa and the dry adiabatic layer above could have served as a ducting mechanism for such waves (Fig. 4b). Why purported gravity waves would have appeared in just this area near Dodge City, whereas the Shirer (1986) model for HCRs predicted the orientation well, is not clear.

b. Development of the rolls

Most of the bands became apparent on radar and satellite imagery (Figs. 2 and 3) in close association with a large-scale region of precipitation that moved from the central Plains to North Carolina, becoming a coastal low-pressure system (e.g., Figs. 1 and 2). This precipitation was related to a vorticity maximum in upper-level northwesterly flow, producing mid- and upper-level ascent and precipitation above the surface anticyclone. The 0000 UTC sounding from Springfield, MO (SGF) had a saturated near-moist-neutral layer above 750 hPa (Fig. 4a). Farther north at Rapid City, SD (RAP), however, the stable layer due to the frontal zone and midtropospheric subsidence was much closer to the ground, reducing the depth of the planetary boundary layer to less than 200 m (Fig. 4a).

In the lower troposphere, the bands developed in association with northerly cold-air advection. Despite this cold-air advection, sensible heat flux from the surface kept the boundary layer well-mixed (e.g., Fig. 4b). In Oklahoma, both the Atmospheric Radiation Measurement (ARM) Program and some Oklahoma Mesonet stations (Brock et al. 1995; Shafer et al. 2000) have sensors to measure the surface heat flux. During much of the time that bands occurred in central Oklahoma, upward instantaneous sensible heat flux from several of these stations ranged from 10 to 50 W m^{-2} (not shown). At Norman between 0600 and 1100 UTC, the upward sensible heat flux averaged about 15 W m^{-2} (Fig. 5). Although HCRs have occurred over a wide range of sensible heat flux (10–200 W m^{-2}) in the previous literature (Table 1 in Atkinson and Zhang 1996; Weckwerth et al. 1997, 1999), the values observed in this study did fall within this range.

Further evidence for strong heat transfer from the ground to the air comes from Oklahoma Mesonet sites that measure ground temperature. For example, when the bands were first observed on radar over central Oklahoma at 0430 UTC, the ground temperature 5 cm below the native vegetation (TS05) was 1°C and the 1.5-m air temperature (TAIR) at Norman was –7°C, a difference (TS05–TAIR) of 8°C (Fig. 5). By the time the bands disappeared from the radar imagery around sunrise (about 1300 UTC), TS05–TAIR maximized at 11°C (Fig. 5). Thus, there is strong evidence that sensible heat flux from the ground may have favored the development of HCRs by creating an unstable boundary layer. Indeed, the soundings taken during the banding indicate a well-mixed boundary layer (e.g., Figs. 4b,c,d).

Before the bands were observed on radar, either 1) HCRs existed but the environment was too dry to produce any clouds or precipitation, or 2) the planetary boundary layer was too shallow or stable for deep circulations to develop (e.g., RAP in Fig. 4a). Comparing the 0000 and 1200 UTC soundings at Norman (Fig. 4c) explains why the bands eventually formed. Decreasing temperature due to the cold-air advection dramatically lowered the lifting condensation level of a surface parcel from 771 hPa to 914 hPa, while the depth of the planetary boundary layer decreased only slightly by comparison (880 to 918 hPa). Thus, buoyant surface parcels at 1200 UTC were more likely to reach their lifting condensation level before reaching the stable inversion layer. If radiational cooling were able to explain the observed cooling, a nocturnal inversion would be expected at the surface, which was not observed (Fig. 4c). Likewise, the moisture profiles did not change substantially (Fig. 4c), indicating that moistening by the precipitation aloft played a minimal role in lowering the height of the lifting condensation level. Other soundings (not shown) also indicate that, where cold-air advection was able to lower the lifting condensation level of near-surface parcels to less than the depth of the planetary boundary layer, observation of the bands became possible.

These results may explain why HCRs are less frequently observed during the cold season than during the warm season. During the warm season, the increased prevalence of scatterers (e.g., insects; Wilson et al. 1994) implies a greater chance of detecting bands on radar, even in clear, dry air [e.g., see the discussion in Weckwerth et al. (1999, 2165–2166)]. In the present winter case, the circulations needed to produce clouds and precipitation were likely occurring before appearing on satellite and radar, but few scatterers were available to reveal these circulations.

c. Snow production

Although snow was not officially reported in the central United States from the bands, snow was recorded unofficially at an experimental present-weather sensor at the Norman site in the Oklahoma Mesonet. Anecdotes of a dusting of snow in and around Norman were also reported. Four and a half hours of light snow were officially reported at Greenwood, MS (GWO), as one of the bands remained nearly stationary over that site from 1153 to 1623 UTC (Fig. 6a). The Jackson, MS (JAN) sounding from 1200 UTC 23 January was nearly isentropic (well-mixed) from the surface up to 911 hPa (959 m MSL or 858 m AGL) and capped by a strong frontal inversion (Fig. 4d). As noted previously, the depth of the bands was about 660 m AGL, suggesting that the vertical circulation of the HCRs likely encompassed the depth of the surface mixed layer. In addition, the clouds comprising the bands at the top of the planetary boundary layer developed within the favored growth zone for dendritic ice crystals between –12° and –18°C [e.g., Fukuta and Takahashi (1999) and references within]. Longwave-infrared (channel 4) satellite imagery confirms that the cloud-top temperatures of the bands ranged from near –20°C when first revealed from underneath the large-scale precipitation region aloft to –15°C at their southernmost extent (Figs. 3b,c). That nearly all the bands appeared from underneath the large-scale precipitation region aloft (Fig. 2) suggests that seeding of ice crystals from aloft into the bands below may have been important. [For a review of the seeder–feeder process, see Cotton and Anthes (1989, 824–833).] The close relationship between the large-scale precipitation region aloft and the bands is even more apparent from animated satellite imagery (http://www.cimms.ou.edu/~schultz/hcr).

d. Dissipation of the rolls

Despite the widespread occurrence of the bands, 4–11 h after the bands were first observed at a location, they disappeared and no clear signature of organized circulations was apparent in either the radar or satellite imagery. What caused the dissipation of the bands? When the bands were initially apparent on the satellite imagery (Figs. 3b,c), the circulations in the bands likely extended upward to near –20°C. As the bands were advected equatorward, drier air at the surface farther south (e.g., note the low dewpoint temperatures in Fig. 6) became ingested into the circulations. Eventually, cloud tops lowered and dissipated, disappearing from radar and satellite imagery (e.g., Figs. 2d, 3d, 6b).

Whether the circulations comprising the HCRs still existed after the bands disappeared from radar is debatable. It is possible that circulations were maintained, but were dry. It is also possible that the ground cooled sufficiently that the upward sensible heat flux became insufficient to maintain the bands. A third possibility might have occurred over Mississippi, and Alabama, where the bands dissipated within a few hours after sunrise (Figs. 2d, 3d, 6). Solar heating warmed the ground surface, as shown by the rising air temperatures in Fig. 6, thus, destabilizing and deepening the boundary layer. In this case, the rolls may not have been transporting enough heat vertically and the circulations transitioned to open-cellular convection or full three-dimensional turbulence (Krishnamurti 1975; Grossman 1982). Evaluating these different hypotheses further was not possible, given the available data.

e. Other events in 2003

Although these bands were most widespread and apparent on 23 January 2003, similar bands were also observed on radar in central Oklahoma on 16 January 2003 (D. Burgess 2003, personal communication). An even more interesting case of these bands occurred on 26 January 2003 in central Illinois (C. Crosbie 2003, personal communication). In this case, a broad region of snow (Figs. 7a,b) moved southeast, revealing bands underneath (Figs. 7b,c,d). The lower troposphere over Lincoln, IL was eerily similar to that over Springfield, MO for the 23 January case, with a well-mixed surface layer, prominent frontal zone between 850 and 750 hPa and a layer saturated with respect to ice above (Fig. 8). The structure of the Lincoln sounding suggests that ice crystals likely originated in the layer above the frontal zone, while HCRs probably developed below the frontal zone. As for the 23 January event, we hypothesize that the snow grew as it fell into the ascending portions of the HCR circulations below, within the favored temperature regime for the dendritic growth of ice crystals. Such a seeder–feeder process suggests one way to anticipate snow-producing HCRs in the future. These three observations of similar bands over this two-week period (16, 23, and 26 January 2003) suggest that snow-producing HCRs over land during the cold season may be more common than previously thought, if the proper conditions are present.

f. Search for similar banding events in Oklahoma

As a further test of our hypothesis, we constructed a larger number of cases where we might have expected to have seen similar banding situations. Data from the Norman Mesonet station were examined for the nine winters of the existence of the Oklahoma Mesonet (1994–1995 to 2002–2003). Eleven events (Table 2) were identified that met the following criteria: (a) the difference between the ground temperature 5 cm below bare soil (TB05) and TAIR was 12°C or greater,[1] (b) TB05–TAIR≥12°C for more than two hours, and (c) synoptic-scale cold advection occurred. The 12°C threshold was chosen to eliminate events that were not similar to the 23 January 2003 event. The threshold was determined by trial and error and eliminated many cases that simply possessed strong diurnal cycles. That is not to say that cold-advection events did not exist for TB05–TAIR<12°C, but rather a greater fraction of the events above that threshold met all three criteria.

The composite synoptic pattern associated with these 11 events was characterized by a cold-air outbreak from an equatorward-moving anticyclone under upper-level northwesterly flow (Figs. 9a,b), of the type described by Schultz et al. (1997, 1998) and references within. Such a pattern is also consistent with that on 23 January 2003. Composite surface temperature over Oklahoma was about –10°C (Fig. 9c), or about 10°C below normal. Such a synoptic pattern would provide

[1] Note that the ground temperature used to identify these 11 events was TB05 instead of TS05. Had the criterion been TS05–TAIR≥12°C, such conditions would have been met much more frequently than the TB05–TAIR≥12°C criterion. Specifically, TS05–TAIR≥12°C occurs several times per month, often during pronounced overnight cooling in calm conditions. These results suggest that dormant vegetation above the TS05 temperature sensor increased the roughness height and better insulated the ground, thereby reducing the sensible heat flux relative to the temperature sensor over the bare soil (TB05).

similar surface heat fluxes to the 23 January 2003 event, possibly sufficient for the occurrence of HCRs.

Seven of these 11 events displayed no reflectivity patterns from the KTLX WSR-88D radar over central Oklahoma (Table 2). In these events, HCRs may or may not have been present, but, if they existed, they were unable to be detected by the radar. Three more events had bands in the planetary boundary layer, but they either lasted for a short time or originated aloft (Table 2). Only one event possessed widespread banding in the planetary boundary layer (18 January1996). These bands, however, also occurred underneath a precipitation shield, as in the 23 January case. In addition, the orientation of the observed bands was within 20–30° of that predicted by the Shirer (1986) model (Table 2).

Norman soundings for nine of these 11 events possessed a surface mixed-layer between 330–960 m deep (not shown). Of these nine soundings, only one (1200 UTC 18 January 1996) had the height of the lifted condensation level less than the height of the top of the boundary layer, which would have allowed clouds within the planetary boundary layer. Thus, this analysis provides further support for the scenario presented in this paper for the 23 January 2003 snowbands. Although 11 events likely had modest sensible heat fluxes over Oklahoma due to a favorable synoptic-scale pattern, the manifestation of bands on the radar imagery was dependent on two additional critical factors: shallow clouds in the planetary boundary layer and falling ice crystals aloft to seed them.

3. Snowbands caused by lake effect

Although the majority of the bands observed on 23 January 2003 were likely associated with HCRs over land, localized bands downstream of unfrozen lakes also occurred, as discussed by two NWS Area Forecast Discussions. Such lakes included Grand Lake O' The Cherokees in northeast Oklahoma, Table Rock Lake in southern Missouri, and Beaver and Bull Shoals Lakes in northern Arkansas. Particularly interesting was the lake-effect band that formed downstream of Lake Kentucky on the Kentucky–Tennessee border (Figs. 10a,b). The long axes of Lake Kentucky that produced the bands are roughly 40–60 km in length. Earth skin temperature from *GOES-8* longwave infrared (channel 4) imagery suggested that the lake was at least 10°C warmer than the surrounding land (Fig. 10c). Northerly flow occurred along the long axis of this north–south-oriented lake, presumably allowing sufficient moisture to be evaporated from the warm surface of the lake, ascend, produce a cloud (Figs. 10a,b), and be deposited downstream as snow. Such a process would be similar to that which occurs downstream of the much larger Great Lakes (e.g., Niziol 1987; Niziol et al. 1995), downstream of the Great Salt Lake (e.g., Carpenter 1993; Steenburgh et al. 2000; Steenburgh and Onton 2001), and over the ocean during cold-air outbreaks (e.g., Kuettner 1971; Walter 1980; Shirer and Brümmer 1986), where the warm water acts as a large source of thermal energy. In fact, previous observations of lake-effect snows have been reported over lakes with fetches as small as 30–50 km: Lake Tahoe and Pyramid Lake in Nevada (Cairns et al. 2001a,b; Huggins et al. 2001) and Bull Shoals Lake in Arkansas (Wilken 1997).

The lake-effect band over Lake Kentucky appeared to have had two phases: a narrow band early in the morning (Fig. 10a) and a broader band later (Figs. 10b,d), about two hours after the snowbands likely associated with the HCRs had dissipated. Previous studies have shown that single narrow lake-effect bands can form when the nighttime land breeze helps focus convergence over the water during a lake-effect event (Peace and Sykes 1966; Passarelli and Braham 1981; Steenburgh and Onton 2001). Such a process might have occurred in this event over Lake Kentucky: as the land breeze dissipated after sunrise, the convergence weakened and the single band became less well defined. Unfortunately, this hypothesis could not be tested because of the sparse surface observations.

4. Conclusion

This paper presents a case of banded snow showers over the central and southeastern United States during the cold-air outbreak of 23 January 2003. Widespread banding occurred likely due to horizontal convective rolls (HCRs), whereas localized banding occurred downstream of some lakes due to lake-effect processes. The bands were compared to theory and previous observations, in an attempt to describe their formation, characteristics, and dissipation.

Analysis of the event of 23 January 2003, as well as several other events, results in the following proposed schematic for the snowbands likely associated with HCRs over the central and southeastern United States (Fig. 11). Cold-air advection over warm ground led to upward sensible heat fluxes producing a well-mixed planetary boundary layer and presumed HCR circulations. Eventually, clouds formed at the top of the ascending portions of the HCR circulations when the height of the lifting condensation level decreased to within the planetary boundary layer. Ice crystals were inferred to have fallen from a large-scale precipitation region aloft associated with midtropospheric ascent, sublimating in the drier air below, but growing in the ascending portions of the HCRs, allowing snow to reach the surface (Fig. 11). As drier air was ingested, the bands dissipated.

In this paper, specialized observations of sensible heat flux and ground temperature (e.g., Fig. 5) were important in supporting our argument that upward heat transfer was likely significant for the occurrence of the bands on 23 January 2003. Numerical weather prediction models have been shown to be quite sensitive to the ground and water temperature. For example, Onton and Steenburgh (2001, section 3f) showed that a simulation of a midlake snowband over the Great Salt Lake was very sensitive to the water temperature, producing about a third more precipitation when the water temperature was increased by only 2°C. A second example from Hjelmfelt and Braham (1983) found that the vertical motions within a lake-effect precipitation band downwind of Lake Michigan was sensitive to the lake temperature, although the precipitation amounts displayed less sensitivity. A third example comes from Powers and Stoelinga (2000) who argued that the accuracy of the surface fluxes may be quite sensitive to the manner in which surface-wave models are coupled to marine-circulation and atmospheric models. Model studies of the sensitivity of precipitation to land-surface temperatures and fluxes are even scarcer because of the lack of verifying observations, indicating the potential for research on this topic. This event highlights the potential importance that having accurate ground- and water-temperature observations is critical for understanding the mechanisms that lead to the formation of these snowbands. That the operational Eta did not produce precipitation in the regions of the snowbands further shows the potential importance of engaged human forecasters, who could recognize the weaknesses in the operational model output, and still generate a useful forecast product.

Acknowledgments. Thanks to those who provided data, assistance, or insight: Mike Baldwin, Philip Bothwell, Harold Brooks, Don Burgess, Casey Crosbie, Roger Edwards, Kim Elmore, Joe Garfield, Janet Martinez, Chris Porter, Matt Wandishin, Louis Wicker, Conrad Ziegler, and three anonymous reviewers. Some of the surface heat flux data were obtained from the Atmospheric Radiation Measurement (ARM) Program sponsored by the Department of Energy, Office of Science, Office of Biological and Environmental Research, Environmental Sciences Division. Funding for Schultz was provided by NOAA/OAR/NSSL under NOAA–OU Cooperative Agreement #NA17RJ1227.

REFERENCES

Agee, E. M., 1976: Observational evidence of cell flatness as a function of convective depth and cell anisotropy. *J. Meteor. Soc. Japan,* **54,** 68–71.

Asai, T., 1970: Stability of a plane parallel flow with variable vertical shear and unstable stratification. *J. Meteor. Soc. Japan,* **48,** 129–139.

Atkinson, B. W., and J. W. Zhang, 1996: Mesoscale shallow convection in the atmosphere. *Rev. Geophys.* **34,** 403–431.

Atlas, D., S.-H. Chou, and W. P. Byerly, 1983: The influence of coastal shape on winter mesoscale air-sea interaction. *Mon. Wea. Rev.,* **111,** 245–252.

Brock, F. V., K. C. Crawford, R. L. Elliott, G. W. Cuperus, S. J. Stadler, H. L. Johnson, and M. D. Eilts, 1995: The Oklahoma Mesonet: A technical overview. *J. Atmos. Ocean. Tech.,* **12,** 5–19.

Brown, R. A., 1980: Longitudinal instabilities and secondary flows in the planetary boundary layer: A review. *Rev. Geophys. Space Phys.,* **18,** 683–697.

Cairns, M. M., R. Collins, T. Cylke, M. Deutschendorf, and D. Mercer, 2001a: A lake effect snowfall in western Nevada---Part I: Synoptic setting and observations. Preprints, *18th Conf. Weather Analysis and Forecasting,* Fort Lauderdale, FL, Amer. Meteor. Soc., 329–332.

Cairns, M. M., J. Corey, and D. R. Koracin, 2001b: A numerical simulation of a rare lake-effect snowfall in western Nevada. Preprints, *18th Conf. Weather Analysis and Forecasting,* Fort Lauderdale, FL, Amer. Meteor. Soc., J62–J64.

Carpenter, D. M., 1993: The lake effect of the Great Salt Lake: Overview and forecast problems. *Wea. Forecasting,* **8,** 181–193.

Chang, H.-R., and H. N. Shirer, 1984: Transitions in shallow convection: An explanation for lateral cell expansion. *J. Atmos. Sci.,* **41,** 2334–2346.

Clark, T. L., T. Hauf, and J. P. Kuettner, 1986: Convectively forced internal gravity waves: Results from two-dimensional numerical experiments. *Quart. J. Roy. Met. Soc.,* **112,** 899–925.

Cotton, W. R., and R. A. Anthes, 1989: *Storm and Cloud Dynamics.* Academic Press, 883 pp.

Fukuta, N., and T. Takahashi, 1999: The growth of atmospheric ice crystals: A summary of findings in vertical supercooled cloud tunnel studies. *J. Atmos. Sci.,* **56,** 1963–1979.

Grossman, R. L., 1982: An analysis of vertical velocity spectra obtained in the BOMEX fair-weather, trade-wind boundary layer. *Bound.-Layer Meteor.,* **23,** 323–357.

Helfand, H. M., and E. Kalnay, 1983: A model to determine open or closed cellular convection. *J. Atmos. Sci.,* **40,** 631–650.

Hjelmfelt, M. R., and R. R. Braham, Jr., 1983: Numerical simulation of the airflow over Lake Michigan for a major lake-effect snow event. *Mon. Wea. Rev.,* **111,** 205–219.

Holroyd, E. W., 1971: Lake-effect cloud bands seen from weather satellites. *J. Atmos. Sci.,* **28,** 1165–1170.

Huggins, A. W., D. E. Kingsmill, and M. M. Cairns, 2001: A lake effect snowfall in western Nevada---Part II: Radar characteristics and quantitative precipitation estimates. Preprints, *18th Conf. Weather Analysis and Forecasting,* Fort Lauderdale, FL, Amer. Meteor. Soc., 333–337.

Kain, J. S., P. R. Janish, S. J. Weiss, M. E. Baldwin, R. S. Schneider, and H. E. Brooks, 2003: Collaboration between forecasters and research scientists at the NSSL and SPC. *Bull. Amer. Meteor. Soc.,* in press. [Available from http://www.nssl.noaa.gov/mag/pubs/BAMS_paper.pdf.]

Kalnay, E., and Coauthors, 1996: The NCEP/NCAR 40-year Reanalysis Project. *Bull. Amer. Meteor. Soc.,* **77,** 437–471.

Kelly, R. D., 1982: A single Doppler radar study of horizontal-roll convection in a lake-effect snow storm. *J. Atmos. Sci.,* **39,** 1521–1531.

Kelly, R. D., 1984: Horizontal roll and boundary-layer interrelationships observed over Lake Michigan. *J. Atmos. Sci.,* **41,** 1816–1826.

Krishnamurti, R., 1975: On cellular cloud patterns. Part 1: Mathematical model. *J. Atmos. Sci.,* **32,** 1353–1363.

Kristovich, D. A. R., 1993: Mean circulations of boundary-layer rolls in lake-effect snow storms. *Bound.-Layer Meteor.,* **63,** 293–315.

Kuettner, J., 1937: Die atmosphärischen Gleichgewichts-Verhältnisse über Lappland im Polarsommer. *Beitr. Phys. Atmos.,* **24,** 98–114.

Kuettner, J., 1959: The band structure of the atmosphere. *Tellus,* **11,** 267–294.

Kuettner, J., 1971: Cloud bands in the earth's atmosphere: Observations and theory. *Tellus,* **23,** 404–425.

Kuettner, J., P., P. A. Hildebrand, and T. L. Clark, 1987: Convection waves: Observations of gravity wave systems over convectively active boundary layers. *Quart. J. Roy. Met. Soc.,* **113,** 445–467.

Kuo, H. L., 1963: Perturbations of plane Couette flow in stratified fluid and origin of cloud streets. *Phys. Fluids,* **6,** 195–211.

LeMone, M. A., and R. J. Meitín, 1984: Three examples of fair-weather mesoscale boundary-layer convection in the Tropics. *Mon. Wea. Rev.,* **112,** 1985–1997.

Ligda, M. G. H., and S. G. Bigler, 1958: Radar echoes from a cloudless cold front. *J. Meteor.,* **15,** 494–501.

Maletzke, R., 1953: Die meteorologischen Vorbedingungen des 1000 km Segelflugs. *Schweizer Aero Revue,* **28,** 191.

Miura, Y., 1986: Aspect ratios of longitudinal rolls and convection cells observed during cold air outbreaks. *J. Atmos. Sci.,* **43,** 29–39.

Niziol, T. A., 1987: Operational forecasting of lake effect snowfall in western and central New York. *Wea. Forecasting,* **2,** 310–321.

Niziol, T. A., W. R. Snyder, and J. S. Waldstreicher, 1995: Winter weather forecasting throughout the eastern United States. Part IV: Lake effect snow. *Wea. Forecasting,* **10,** 61–77.

Onton, D. J., and W. J. Steenburgh, 2001: Multiscale analysis of the 7 December 1998 Great Salt Lake-effect snowstorm. *Mon. Wea. Rev.,* **129,** 1318–1338.

Passarelli, R. E., Jr., and R. R. Braham Jr., 1981: The role of the winter land breeze in the formation of Great Lake snow storms. *Bull. Amer. Meteor. Soc.,* **62,** 482–491.

Peace, R. L., and R. B. Sykes Jr., 1966: Mesoscale study of a lake-effect snowstorm. *Mon. Wea. Rev.,* **94,** 495–507.

Powers, J. G., and M. T. Stoelinga, 2000: A coupled air–sea mesoscale model: Experiments in atmospheric sensitivity to marine roughness. *Mon. Wea. Rev.,* **128,** 208–228.

Sasaki, Y., 1970: Influences of thermal boundary layer on atmospheric cellular convection. *J. Meteor. Soc. Japan*, **48,** 492–502.

Schultz, D. M., and P. N. Schumacher, 1999: The use and misuse of conditional symmetric instability. *Mon. Wea. Rev.,* **127,** 2709–2732; Corrigendum, **128,** 1573.

Schultz, D. M., W. E. Bracken, L. F. Bosart, G. J. Hakim, M. A. Bedrick, M. J. Dickinson, and K. R. Tyle, 1997: The 1993 Superstorm cold surge: Frontal structure, gap flow, and tropical impact. *Mon. Wea. Rev.,* **125,** 5–39; Corrigenda, **125,** 662.

Schultz, D. M., W. E. Bracken, and L. F. Bosart, 1998: Planetary- and synoptic-scale signals associated with Central American cold surges. *Mon. Wea. Rev.,* **126,** 5–27.

Shafer, M. A., C. A. Fiebrich, D. Arndt, S. E. Fredrickson, and T. W. Hughes, 2000: Quality assurance procedures in the Oklahoma Mesonetwork. *J. Atmos. Ocean. Tech.,* **17,** 474–494.

Shirer, H. N., 1986: On cloud street development in three dimensions: Parallel and Rayleigh instabilities. *Contrib. Atmos. Phys.,* **59,** 126–149.

Shirer, H. N., and B. Brümmer, 1986: Cloud streets during KonTur: A comparison of parallel/thermal instability modes with observations. *Contrib. Atmos. Phys.,* **59,** 150–161.

Steenburgh, W. J., S. F. Halvorson, and D. J. Onton, 2000: Climatology of lake-effect snowstorms of the Great Salt Lake. *Mon. Wea. Rev.,* **128,** 709–727.

Steenburgh, W. J., and D. J. Onton, 2001: Multiscale analysis of the 7 December 1998 Great Salt Lake-effect snowstorm. *Mon. Wea. Rev.,* **129,** 1296–1317.

Walter, B. A. 1980: Wintertime observations of roll clouds over the Bering Sea. *Mon. Wea. Rev.,* **108,** 2024–2031.

Weckwerth, T. M., J. W. Wilson, R. M. Wakimoto, and N. A. Crook, 1997: Horizontal convective rolls: Determining the environmental conditions supporting their existence and characteristics. *Mon Wea. Rev.,* **125,** 505–526.

Weckwerth, T. M., T. W. Horst, and J. W. Wilson, 1999: An observational study of the evolution of horizontal convective rolls. *Mon. Wea. Rev.,* **127,** 2160–2179.

Wilken, G. R., 1997: A lake-effect snow in Arkansas. NWS Southern Region Tech. Attach. SR/SSD 97-21, 5 pp. [Available at http://www.srh.noaa.gov/ftproot/topics/attach/html/ssd97-21.htm.]

Wilson, J. W., T. M. Weckwerth, J. Vivekanandan, R. M. Wakimoto, and R. W. Russell, 1994: Boundary-layer clear-air radar echoes: Origins of echoes and accuracy of derived winds. *J. Atmos. Ocean. Tech.,* **11,** 1184–1206.

Young, G. S., D. A. R. Kristovich, M. R. Hjelmfelt, and R. C. Foster, 2003: Rolls, streets, waves, and more. A review of quasi-two-dimensional structures in the atmospheric boundary layer. *Bull. Amer. Meteor. Soc.,* **83,** 997–1001, ES54–ES69.

TABLE LIST

Table 1. A comparison of the observed orientation of the bands to that predicted by the Shirer (1986) model with Coriolis parameter set to zero (his equation 3.13). The observed band orientation is determined by visual inspection of the radar imagery at the stated time and location. Winds used in the model are determined from the closest sounding in time and space, listed in the table. Winds used in the model are from the surface to cloud base or the top of the boundary layer, whichever is lower. The orientation angles in the table below are in standard meteorological convention (0° is north, with positive values denoting angles east of north and negative values denoting angles west of north). The Shirer (1986) model predicts the orientation in standard mathematical notation (0° is east, with positive values denoting angles north of east and negative values denoting angles south of east), which have been converted into standard meteorological convention for comparison to the observed orientation angles.

Table 2. Periods meeting the following criteria at the Norman Oklahoma Mesonet site during the winters of 1995–1996 to 2002–2003: (i) the difference between the ground temperature 5 cm below bare soil (TB05) and the 1.5-m air temperature (TAIR) was 12°C or greater, (ii) this difference lasted for more than two hours, and (iii) synoptic-scale cold advection occurred. Band orientation for events that produced bands is predicted from the Shirer (1986) model, as discussed in Table 1.

Table 1. A comparison of the observed orientation of the bands to that predicted by the Shirer (1986) model with Coriolis parameter set to zero (his equation 3.13). The observed band orientation is determined by visual inspection of the radar imagery at the stated time and location. Winds used in the model are determined from the closest sounding in time and space, listed in the table. Winds used in the model are from the surface to cloud base or the top of the boundary layer, whichever is lower. The orientation angles in the table below are in standard meteorological convention (0° is north, with positive values denoting angles east of north and negative values denoting angles west of north). The Shirer (1986) model predicts the orientation in standard mathematical notation (0° is east, with positive values denoting angles north of east and negative values denoting angles south of east), which have been converted into standard meteorological convention for comparison to the observed orientation angles.

Radar Time (UTC)	Sounding Time (UTC)	Radar Location	Sounding Location	Predicted Orientation Angle (°)	Observed Orientation Angle (°)
2258 22 Jan.	0000 23 Jan.	Dodge City, KS (KDDC)	Dodge City, KS (DDC)	72	90
2258 22 Jan.	0000 23 Jan.	Wichita, KS (KICT)	Topeka, KS (TOP)	23	40
0956 23 Jan.	1200 23 Jan.	Hytop, AL (KHTX)	Birmingham, AL (BMX)	1	342
1152 23 Jan.	1200 23 Jan.	Jackson, MS (KDGX)	Jackson, MS (JAN)	18	7

Table 2. Periods meeting the following criteria at the Norman Oklahoma Mesonet site during the winters of 1995–1996 to 2002–2003: (i) the difference between the ground temperature 5 cm below bare soil (TB05) and the 1.5-m air temperature (TAIR) was 12°C or greater, (ii) this difference lasted for more than two hours, and (iii) synoptic-scale cold advection occurred. Band orientation for events that produced bands is predicted from the Shirer (1986) model, as discussed in Table 1.

Date	**Radar observations of bands, if any**
0915–1415 UTC 9 February 1994	no bands; precipitation south of radar
0430–1615 UTC 18 January 1996	widespread bands underneath elevated precipitation
	band orientation: predicted: 193° vs observed: 157–175°
0515–1600 UTC 31 January 1996	no bands; weak radar echoes never reached surface
0630–1345 UTC 4 February 1996	no bands; no echoes
0800–1015 UTC 9 March 1996	bands present in elevated precipitation
	band orientation: predicted: 132° vs observed: 152–167°
0130–0515 UTC 25 March 1996	few bands very weak and shortlived
	band orientation: predicted: 125° vs observed: 153–164°
0700–1530 UTC 28 January 1997	no bands; no echoes
0900–1515 UTC 3 January 1999	no bands; no echoes
0600–1345 UTC 3 March 2002	no bands; no echoes
1000–1430 UTC 7 February 2003	no bands; no echoes
0445–1545 UTC 24 February 2003	bands present underneath elevated precipitation
	band orientation: predicted: 51° vs observed: 59°

FIGURE LIST

Figure 1: Surface map from NOAA/NCEP/Hydrometeorological Prediction Center at 1200 UTC 23 January 2003. A full-resolution image of this figure can be found at http://www.cimms.ou.edu/~schultz/hcr/paper/Fig1.pdf.

Figure 2: Unfiltered, 0.5° elevation angle, radar reflectivity factor (dB*Z*) from the nationwide WSR-88D network: (a) 2346 UTC 22 January, (b) 0604 UTC 23 January, (c) 1152 UTC 23 January, and (d) 1515 UTC 23 January. Locations of stations mentioned in the text are identified: TOP=Topeka, KS; ICT=Wichita, KS; DDC=Dodge City, KS; SGF=Springfield, MO; OUN=Norman, OK; KHTX=Hytop, AL; BMX=Birmingham, AL; KDGX/JAN=Jackson, MS. For an animation of this imagery, see http://www.cimms.ou.edu/~schultz/hcr/.

Figure 3: *GOES-8* 4-km longwave-infrared (channel 4) satellite imagery for 23 January 2003: (a) 0015 UTC, (b) 0615 UTC, (c) 1145 UTC, and (d) 1515 UTC. Color enhancement scale for brightness temperature (°C) at bottom right of each panel. For an animation of this imagery, see http://www.cimms.ou.edu/~schultz/hcr/.

Figure 4: Skew-*T*–log *p* plots of temperature (solid lines) and dewpoint temperature (dashed lines) for 23 January (a) Springfield, MO (black lines) and Rapid City, SD (gray lines) at 0000 UTC, (b) Dodge City, KS (DDC) at 0000 UTC (black line) , (c) Norman, OK (OUN) at 0000 UTC (black line) and 1200 UTC (gray line), and (d) Jackson, MS (JAN) at 1200 UTC (black line). Pennant, barb, and half-barb represent wind speeds of 25, 5, and 2.5 m s^{-1}, respectively.

Figure 5: Observed 1.5-m air temperature (°C, thick black line), 5-cm soil temperature below native vegetation (°C, thick gray line), and estimated sensible heat flux (W m^{-2}, thin gray line) at the Norman Oklahoma Mesonet station on 23 January 2003. Vertical gray lines at 0430 and 1300 UTC denote the period during when bands were apparent on central Oklahoma WSR-88D radars.

Figure 6: Visible satellite imagery from *GOES-8* over Mississippi and Alabama at (a) 1445 UTC 23 January 2003 and (b) 1632 UTC 23 January 2003. Surface temperature (°F, red), surface dewpoint (°F, green), and surface wind (yellow; pennant, barb, and half-barb represent wind speeds of 25, 5, and 2.5 m s^{-1}, respectively). GWO=Greenwood, MS; JAN=Jackson, MS. For an animation of this imagery, see http://www.cimms.ou.edu/~schultz/hcr/.

Figure 7: The 0.5° elevation angle, radar reflectivity factor (dB*Z*) from the Lincoln, IL WSR-88D (KILX) radar on 26 January 2003: (a) 1042 UTC, (b) 1200 UTC, (c) 1249 UTC, and (d) 1456 UTC. For an animation of this imagery, see http://www.cimms.ou.edu/~schultz/hcr/.

Figure 8: Skew-*T*–log *p* plot of temperature (solid lines) and dewpoint temperature (dashed lines) for 0000 UTC 23 January 2003 Springfield, MO (black lines) and 1200 UTC 26 January 2003 Lincoln, IL (gray lines). Pennant, barb, and half-barb represent wind speeds of 25, 5, and 2.5 m s^{-1}, respectively.

Figure 9: Composite fields from NCEP/NCAR Reanalysis (Kalnay and Coauthors 1996) of (a) mean sea level pressure (hPa), (b) 500-hPa geopotential height (dam), and (c) surface

temperature (°C) for the 11 events in Table 2. Images adapted from those provided by the NOAA–CIRES Climate Diagnostics Center, Boulder Colorado, from their Web site at http://www.cdc.noaa.gov/.

Figure 10: *GOES-8* satellite imagery over Kentucky and Tennessee at 1415 UTC 23 January 2003 [(a) and (c)] and 1732 UTC 23 January 2003 [(b) and (d)]. 1-km visible imagery [(a) and (b)] and 4-km longwave-infrared (channel 4) imagery [(c) and (d)]. The narrow lake-effect bands cannot be identified in (c) because of inadequate resolution of the imagery and/or cloud-top temperature being nearly equal to the Earth's skin temperature. For an animation of this imagery, see http://www.cimms.ou.edu/~schultz/hcr/.

Figure 11: Schematic vertical cross section illustrating proposed mechanism for seeding of snow-producing cloud bands produced by HCRs. Clouds represented by gray scalloped lines. Large snowflakes represent light to moderate snow. Small snowflakes represent sublimating snow. Dashed ovals with arrows represent circulation of HCRs. LCL=lifting condensation level; PBL=planetary boundary layer.

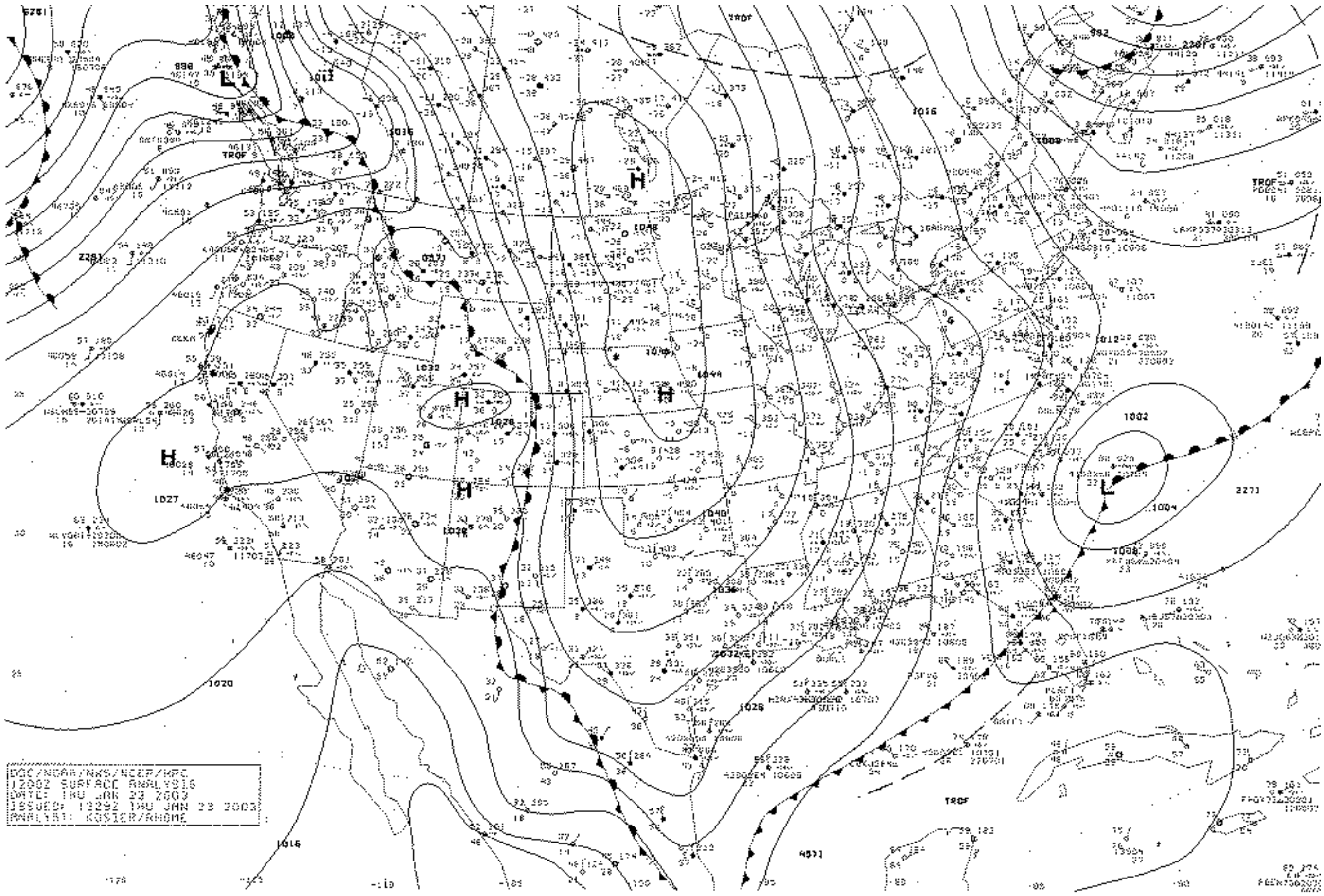

Figure 1: Surface map from NOAA/NCEP/Hydrometeorological Prediction Center at 1200 UTC 23 January 2003.

A full-resolution image of this figure can be found at http://www.cimms.ou.edu/~schultz/hcr/paper/Fig1.pdf.

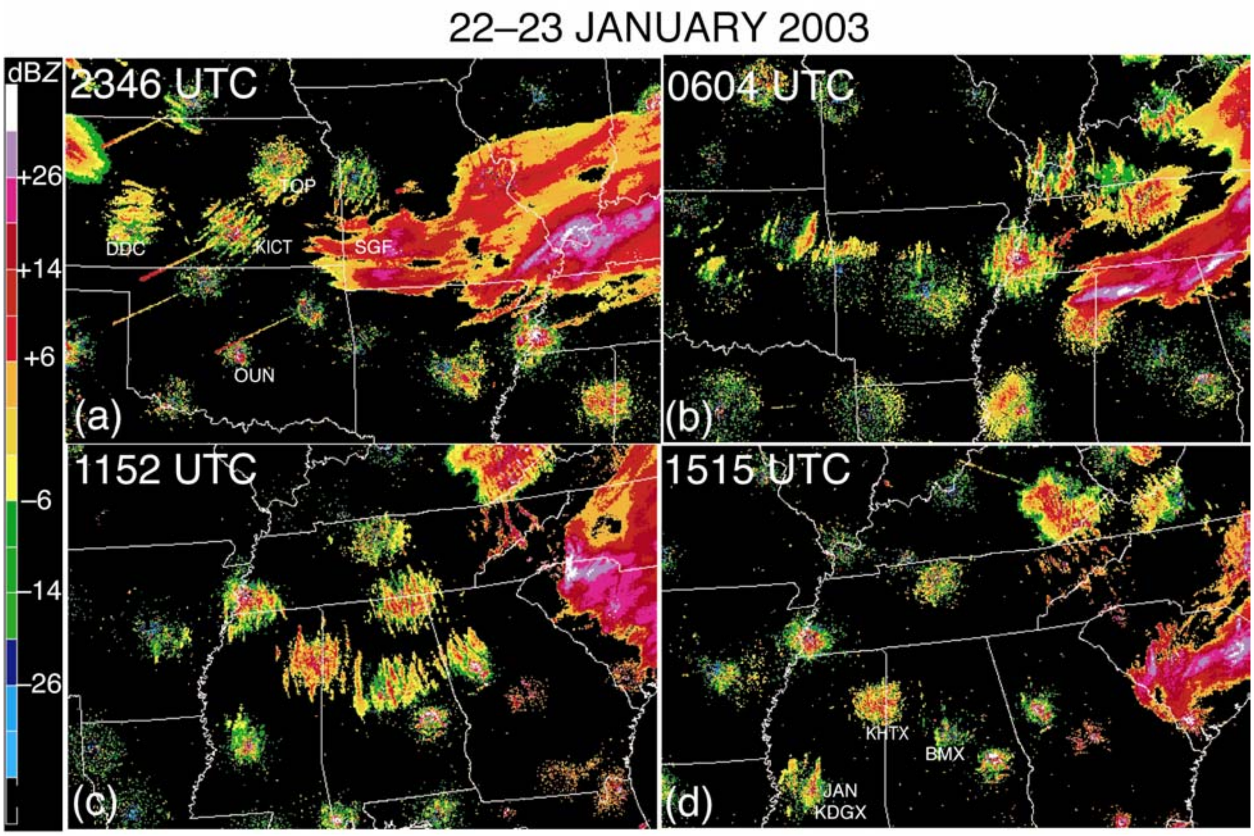

Figure 2: Unfiltered, 0.5° elevation angle, radar reflectivity factor (dB*Z*) from the nationwide WSR-88D network: (a) 2346 UTC 22 January, (b) 0604 UTC 23 January, (c) 1152 UTC 23 January, and (d) 1515 UTC 23 January. Locations of stations mentioned in the text are identified: TOP=Topeka, KS; ICT=Wichita, KS; DDC=Dodge City, KS; SGF=Springfield, MO; OUN=Norman, OK; KHTX=Hytop, AL; BMX=Birmingham, AL; KDGX/JAN=Jackson, MS. For an animation of this imagery, see http://www.cimms.ou.edu/~schultz/hcr/.

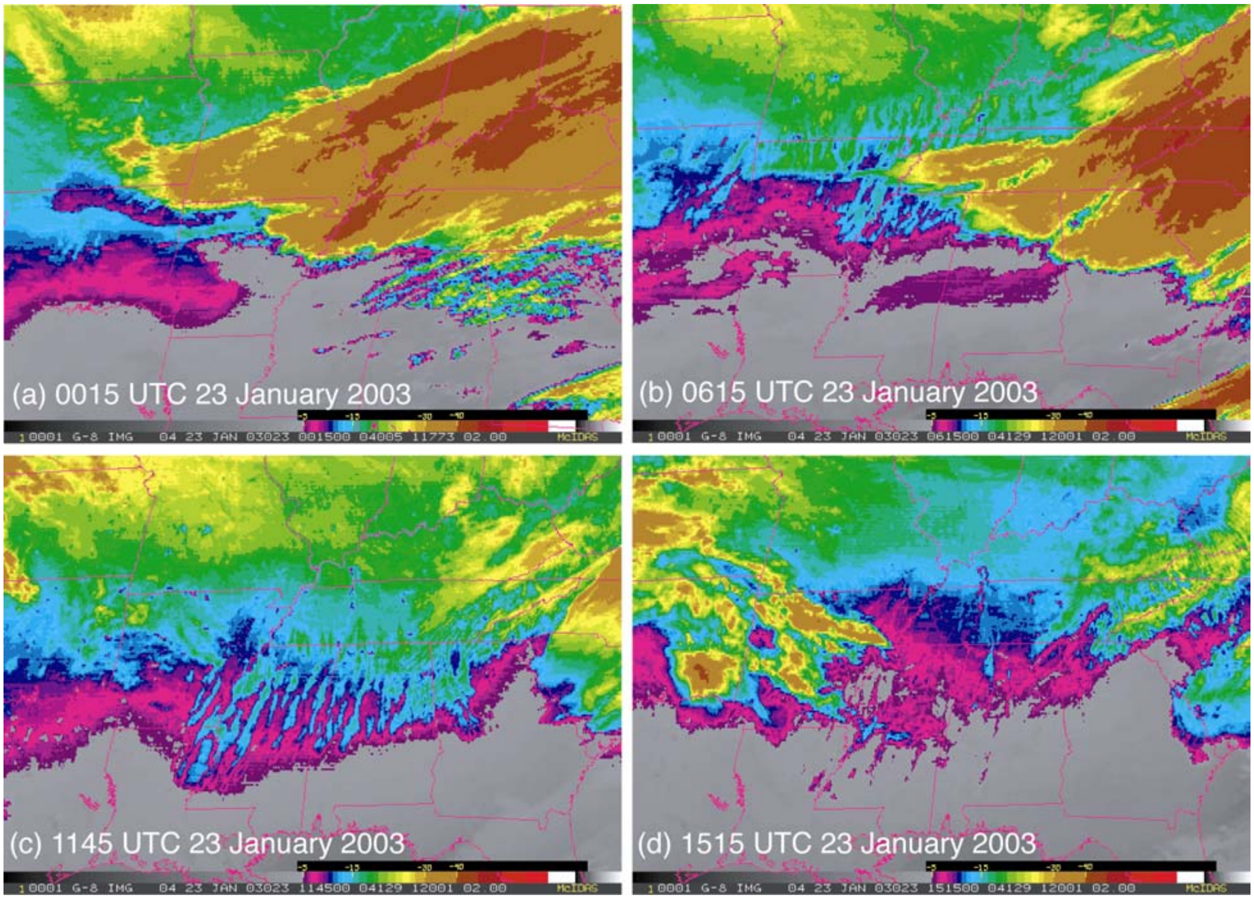

Figure 3: *GOES-8* 4-km longwave-infrared (channel 4) satellite imagery for 23 January 2003: (a) 0015 UTC, (b) 0615 UTC, (c) 1145 UTC, and (d) 1515 UTC. Color enhancement scale for brightness temperature (°C) at bottom right of each panel. For an animation of this imagery, see http://www.cimms.ou.edu/~schultz/hcr/.

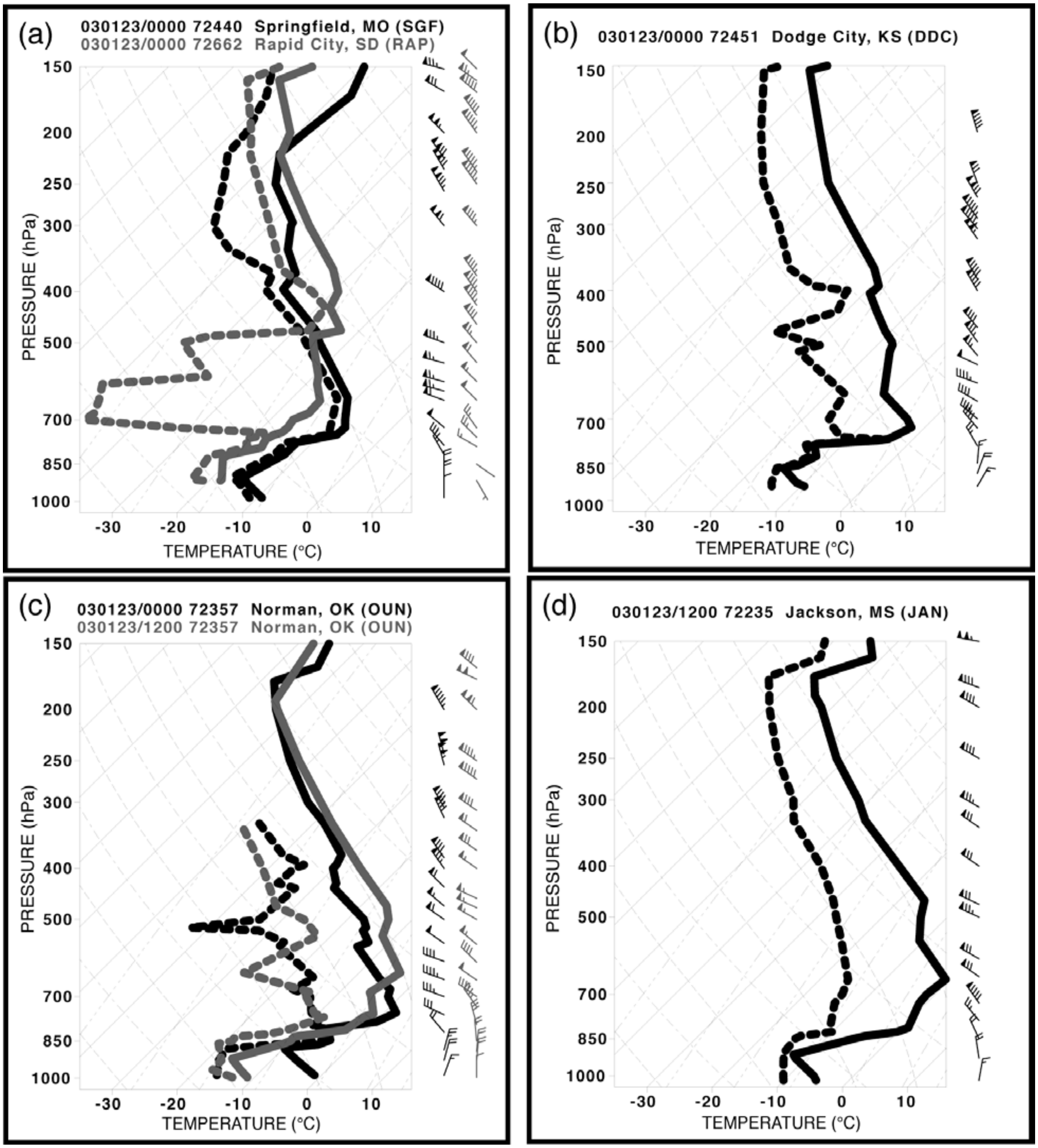

Figure 4: Skew-*T*–log *p* plots of temperature (solid lines) and dewpoint temperature (dashed lines) for 23 January (a) Springfield, MO (black lines) and Rapid City, SD (gray lines) at 0000 UTC, (b) Dodge City, KS (DDC) at 0000 UTC (black line) , (c) Norman, OK (OUN) at 0000 UTC (black line) and 1200 UTC (gray line), and (d) Jackson, MS (JAN) at 1200 UTC (black line). Pennant, barb, and half-barb represent wind speeds of 25, 5, and 2.5 m s^{-1}, respectively.

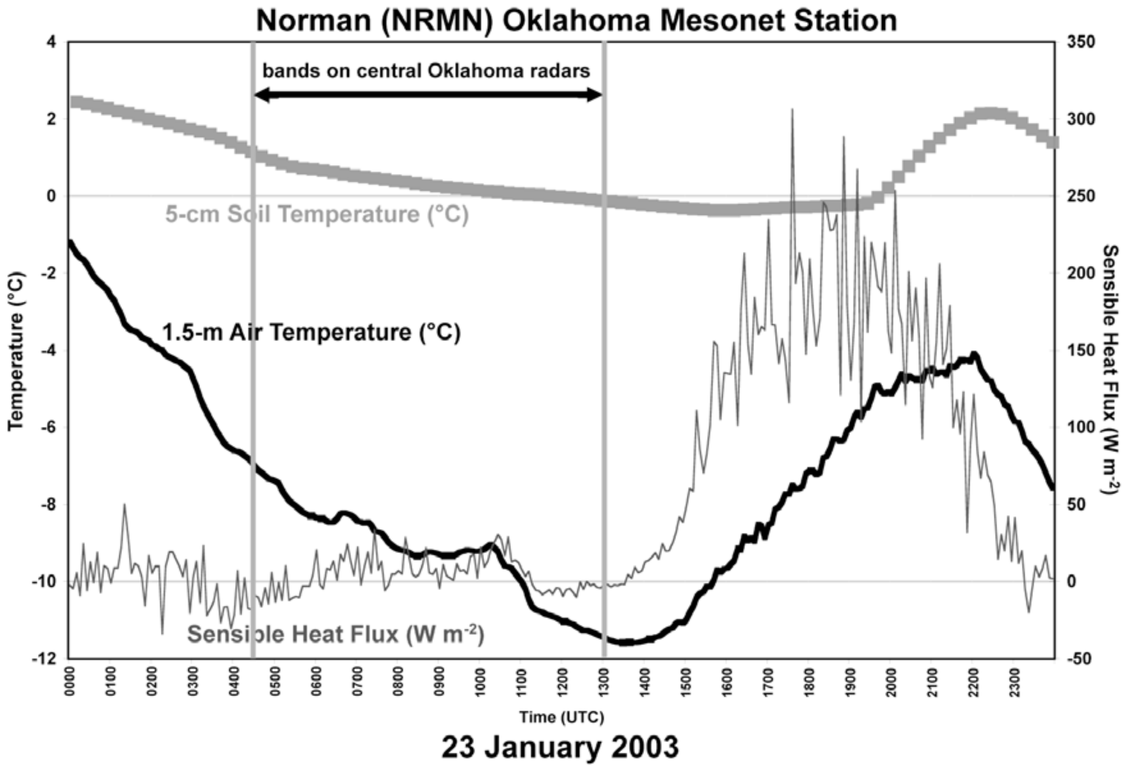

Figure 5: Observed 1.5-m air temperature (°C, thick black line), 5-cm soil temperature below native vegetation (°C, thick gray line), and estimated sensible heat flux (W m^{-2}, thin gray line) at the Norman Oklahoma Mesonet station on 23 January 2003. Vertical gray lines at 0430 and 1300 UTC denote the period during when bands were apparent on central Oklahoma WSR-88D radars.

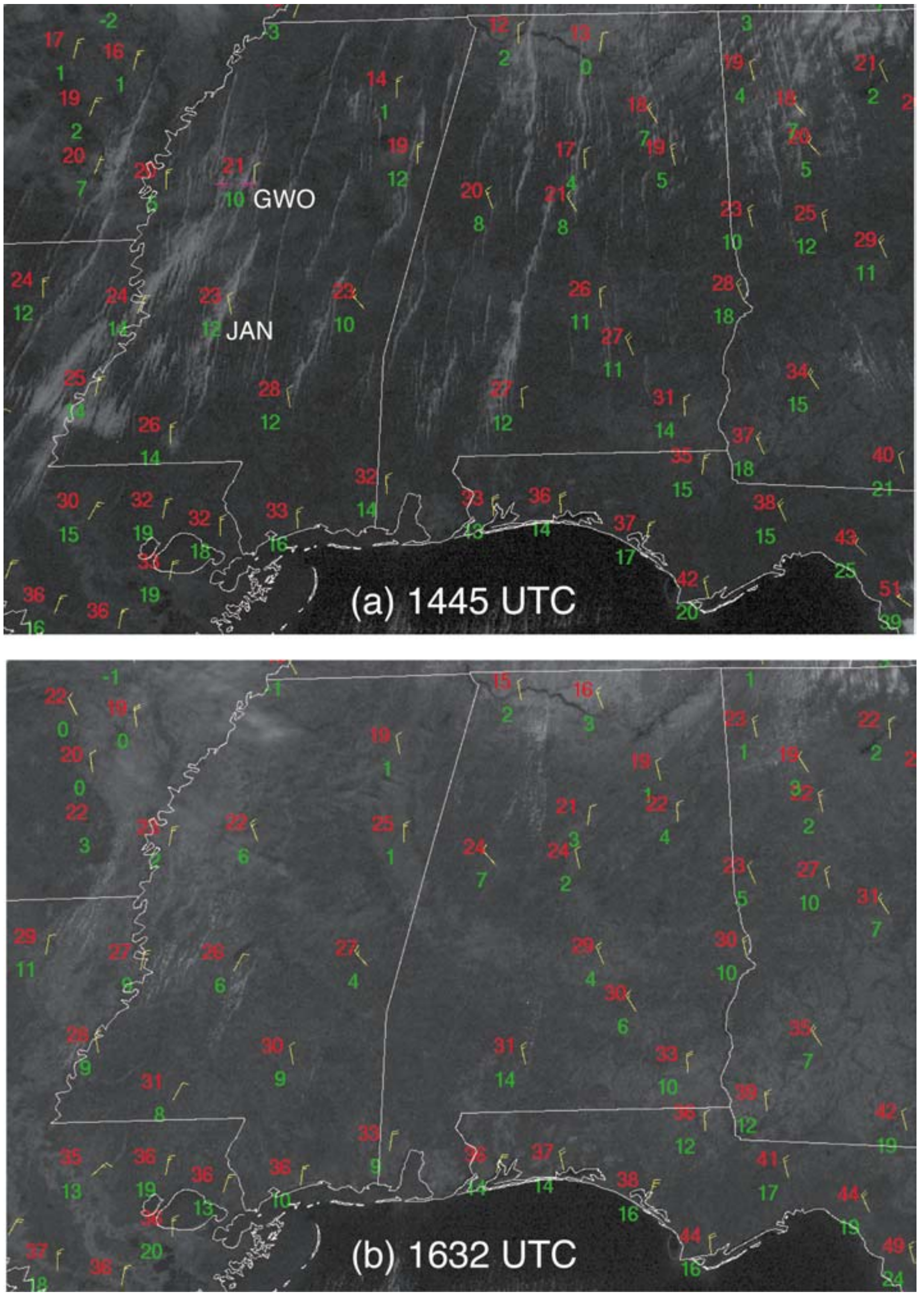

Figure 6: Visible satellite imagery from *GOES-8* over Mississippi and Alabama at (a) 1445 UTC 23 January 2003 and (b) 1632 UTC 23 January 2003. Surface temperature (°F, red), surface dewpoint (°F, green), and surface wind (yellow; pennant, barb, and half-barb represent wind speeds of 25, 5, and 2.5 m s^{-1}, respectively). GWO=Greenwood, MS; JAN=Jackson, MS. For an animation of this imagery, see http://www.cimms.ou.edu/~schultz/hcr/.

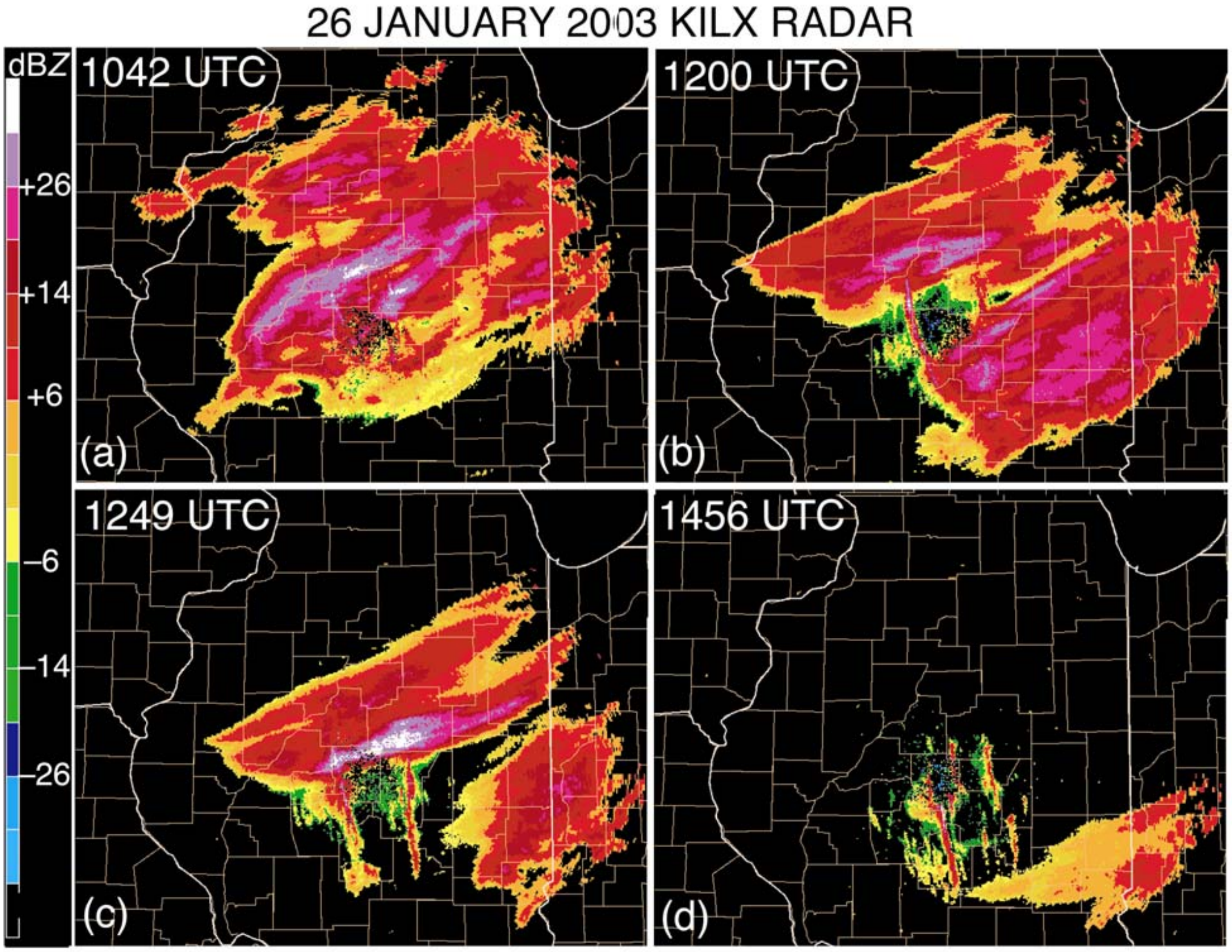

Figure 7: The 0.5° elevation angle, radar reflectivity factor (dB*Z*) from the Lincoln, IL WSR-88D (KILX) radar on 26 January 2003: (a) 1042 UTC, (b) 1200 UTC, (c) 1249 UTC, and (d) 1456 UTC. For an animation of this imagery, see http://www.cimms.ou.edu/~schultz/hcr/.

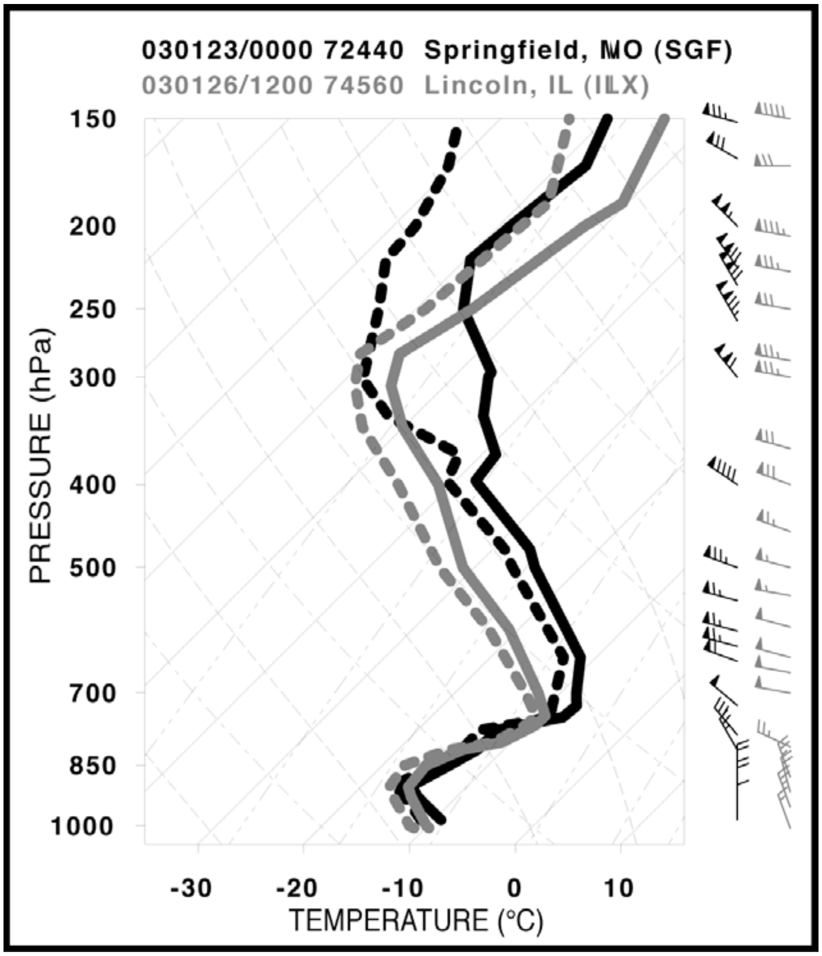

Figure 8: Skew-*T*–log *p* plot of temperature (solid lines) and dewpoint temperature (dashed lines) for 0000 UTC 23 January 2003 Springfield, MO (black lines) and 1200 UTC 26 January 2003 Lincoln, IL (gray lines). Pennant, barb, and half-barb represent wind speeds of 25, 5, and 2.5 m s^{-1}, respectively.

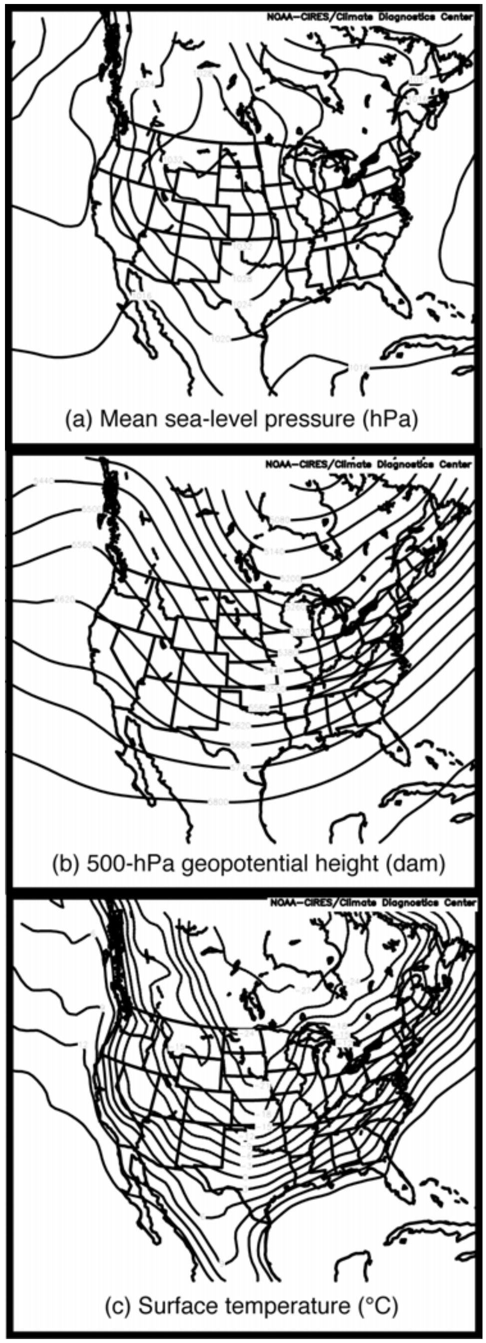

Figure 9: Composite fields from NCEP/NCAR Reanalysis (Kalnay and Coauthors 1996) of (a) mean sea level pressure (hPa), (b) 500-hPa geopotential height (dam), and (c) surface temperature (°C) for the 11 events in Table 2. Images adapted from those provided by the NOAA–CIRES Climate Diagnostics Center, Boulder Colorado, from their Web site at http://www.cdc.noaa.gov/.

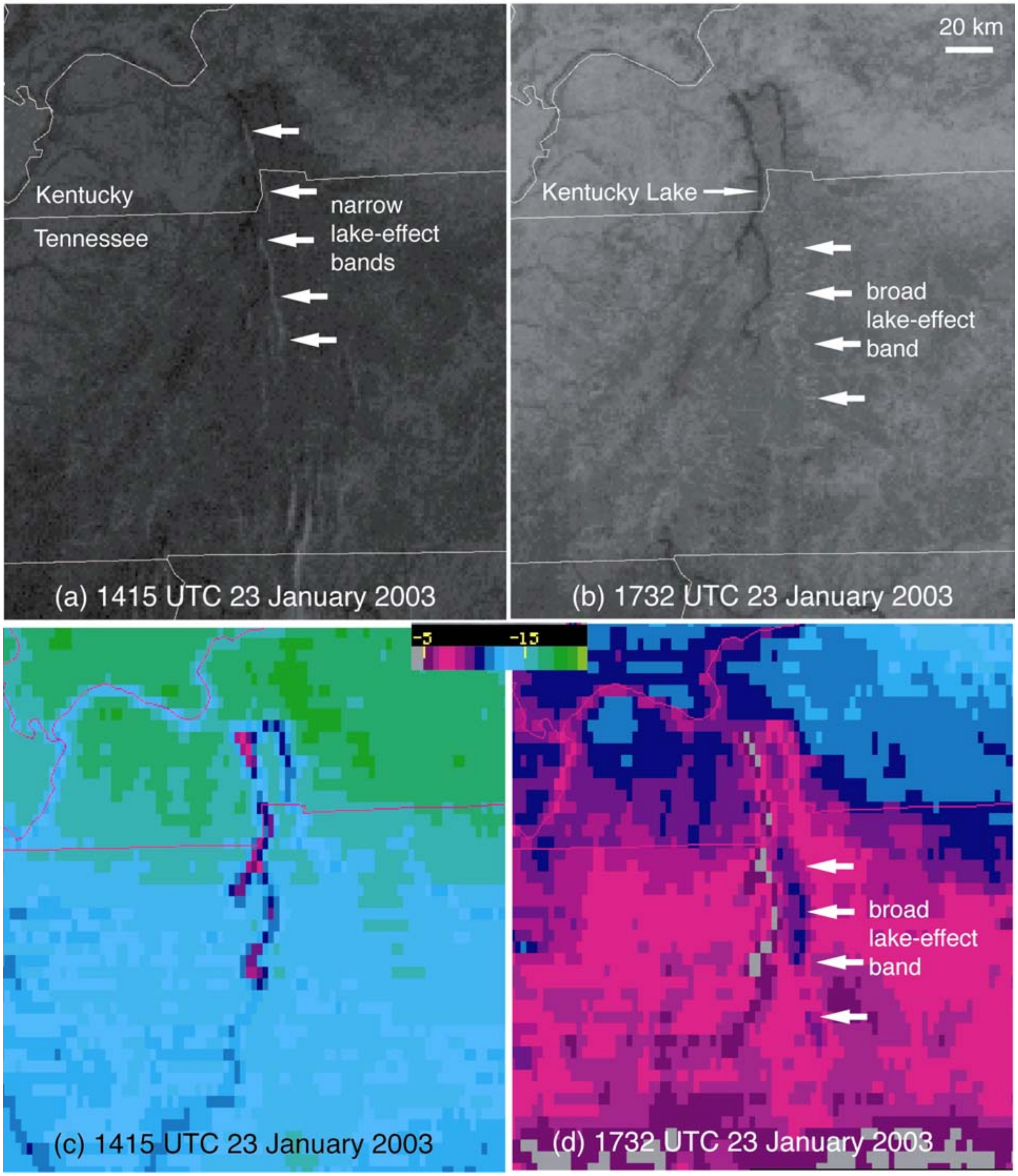

Figure 10: *GOES-8* satellite imagery over Kentucky and Tennessee at 1415 UTC 23 January 2003 [(a) and (c)] and 1732 UTC 23 January 2003 [(b) and (d)]. 1-km visible imagery [(a) and (b)] and 4-km longwave-infrared (channel 4) imagery [(c) and (d)]. The narrow lake-effect bands cannot be identified in (c) because of inadequate resolution of the imagery and/or cloud-top temperature being nearly equal to the Earth's skin temperature. For an animation of this imagery, see http://www.cimms.ou.edu/~schultz/hcr/.

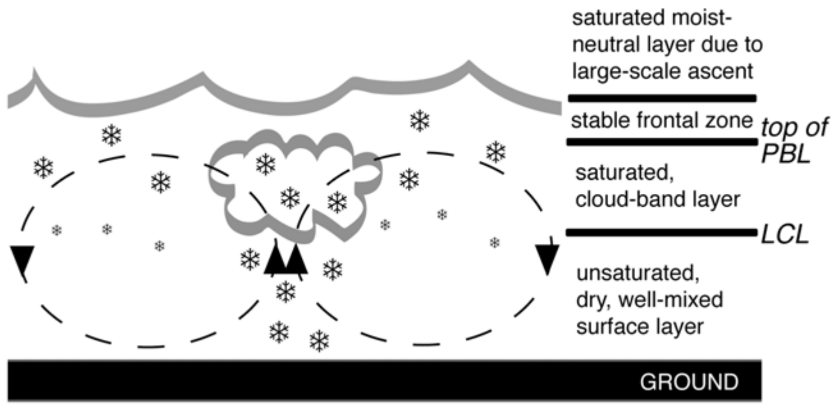

Figure 11: Schematic vertical cross section illustrating seeding of snow-producing cloud bands produced by HCRs. Clouds represented by gray scalloped lines. Large snowflakes represent light to moderate snow. Small snowflakes represent sublimating snow. Dashed ovals with arrows represent circulation of HCRs. LCL=lifting condensation level; PBL=planetary boundary layer.